Electronic Supplementary Material (ESI) for Soft Matter.

Supplementary Material

SOLVENT-FREE AND BIOCOMPATIBLE MULTIPHASED ORGANIC-INORGANIC HYBRID NANOCOMPOSITES

Laura C.E. da Silva[a], Luiz G. L. Germiniani[a], Tomás S. Plivelic[b] and Maria C. Gonçalves[a]

[a] Institute of Chemistry, University of Campinas (UNICAMP), P.O.box 6154, Campinas 13083-970, Brazil

b MAX IV Laboratory, Lund University, P.O box 118, 22100, Lund, Sweden

S1 shows $I(q)xq^2$ versus q plot for peak 1 from which the Invariants (Q^{exp}) were obtained. The intensity curves were obtained from subtracting Peak 2 and 3 intensity contributions as well as the background from the experimental data. Data were normalized by sample thickness.

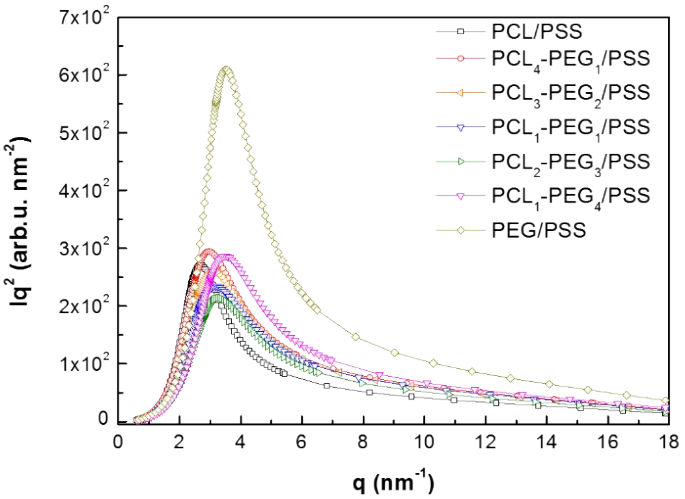

S1– $I(q)q^2$ versus q plots binary and ternary hybrid nanocomposites.

Table S2 presents a summary of the volume fractions used to calculate the contrast differences of these four-phase systems. To achieve adequate estimates, the first step was to convert the mass ratios in volume ratios. For this, the densities of PCL and PEG precursors were measured by conventional picnometry, while the densities of the samples were measured by helium picnometry. The only soluble component in this system is the unbound polymers. Theferore, the soluble fraction (W_s – Table 2, manuscript) is directly converted into the volume fraction of the unbound polymers (Φ_{up}). The difference between the overall polymer volume fraction (PCL+PEG) and Φ_{up} is the cross-linked polymer volume fraction (Φ_{cl}). In order to determine the two remaining volume fractions (Φ_{np},Φ_{sc}), the average atomic ratio, found in the ^{29}Si NMR analysis (Figure 2, manuscript), was converted into volume ratio. For that, it is necessary to assume that all Si atoms present in the cross-linked matrix (silsesquioxane cages) are T^3 type and all Si atoms present in the polysilsesquioxane nanoparticles are T^2 type.

S2 –Volume fractions (ϕ_i) of each phase used in the estimation of the electron density differences (via Eq. 7 and 8).

Sample	Volume fraction			
	ϕ_{up}	ϕ_{cp}	ϕ_{np}	ϕ_{sc}
PEG/PSS	0,082	0,338	0,238	0,348
PCL_1-PEG_4/PSS	0,056	0,374	0,226	0,344
PCL_2-PEG_3/PSS	0,067	0,379	0,220	0,333
PCL_1-PEG_1/PSS	0,140	0,314	0,217	0,329
PCL_3-PEG_2/PSS	0,074	0,387	0,214	0,325
PCL_4-PEG_1/PSS	0,069	0,407	0,208	0,316
PCL/PSS	0,034	0,459	0,169	0,338

up: unbound polymer; cp: cross-linked polymer; np: polysilsesquioxane nanoparticle; sc: silsesquioxane cages.

S3 supplementary material shows the ATR-IR follow-up of the organic polymer chain ends modification and subsequent polysilsesquioxane synthesis. These reactions resulted in binary cross-linked PEG/PSS (left) and PCL/PSS (right) nanocomposites. Briefly, these results show that thechain end modification was successful,which is evidenced by the consumption of the isocyanate group at the propyl end of the alkyltriethoxysilane - 2274 cm^{-1} band (marked yellow); and the carbamate bond formation - 1720 cm^{-1} and 1530 cm^{-1} bands (marked in grey). Polysilsesquioxane formation wasalso successful, as shown by the appearance of multiple bands in the 1110 cm^{-1} to 1050 cm^{-1} region, which are characteristicof Si-O-Si bond asymmetric stretching. The disappearance of the 950 $cm^{-1}$and 775 cm^{-1}bands (marked in grey) show that ethoxy pendant groups were removed, while the small broad band in 905 cm^{-1}, which is attributed to silanol groups, shows that even though ethoxy groups were successfully hydrolyzed to silanol, silanol condensation was not complete.

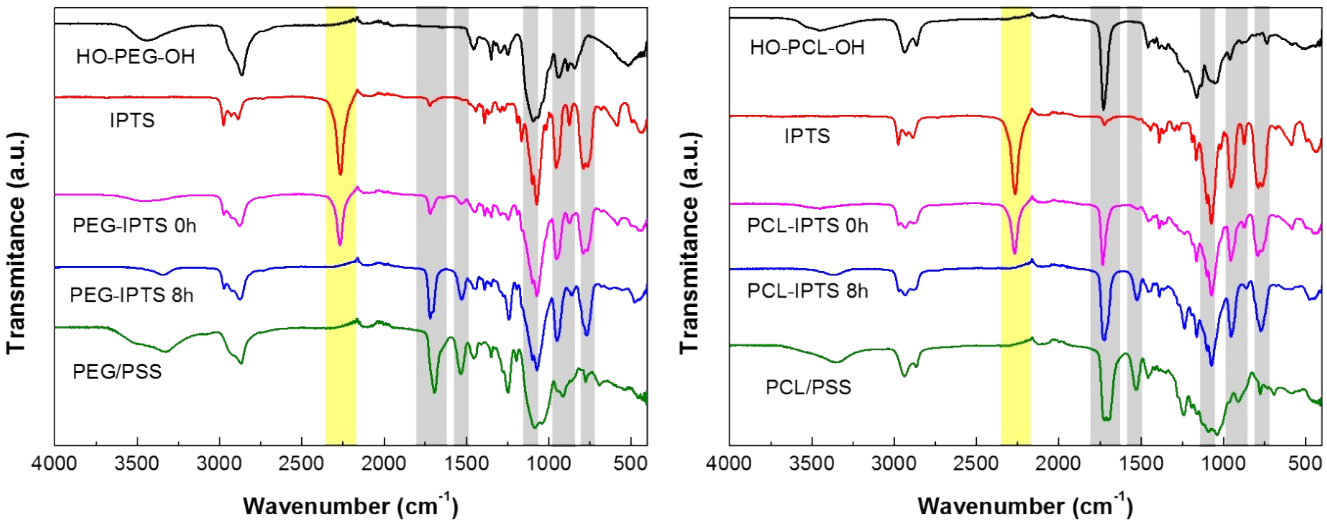

S3–Attenuated total reflectance infrared spectra of the organic precursors (black), (3-isocianatopropyl) triethoxysilane (IPTES) (red),chemically modified PEG (left) and PCL (right), before (pink) and after (blue) the modification reaction andthe organic-inorganic hybrid nanocomposites (green).Bands highlighted in yellow are characteristic of isocyanate groups, while bands highlighted in grey are characteristic of carbamate groups and polysilsesquioxane.

S4 supplementary material shows the photograph of the chemically cross-linked nanocomposites synthesized in this work. It is possible to verify that even though all the materials are transparent, they present air bubbles visible to the naked eye. Air bubbles are formed by ethanol evolution during polysilsesquioxane formation.

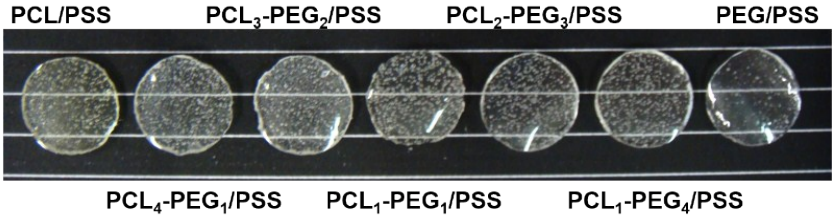

S4–Photograph of the chemically cross-linked nanocomposites synthesized in this work.

S5 supplementary material shows the DSC curves of the binary and ternary chemically cross-linked nanocomposites. All chemically cross-linked nanocomposites are amorphous.

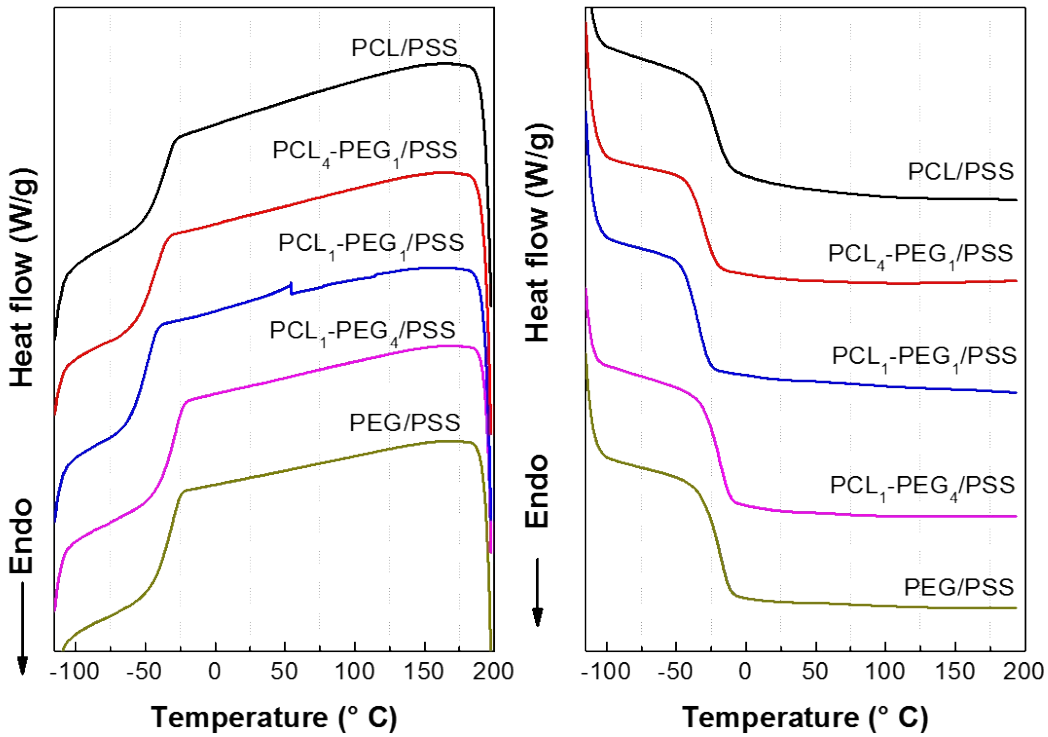

S5– Differential scanning calorimetry of the binary and ternary chemically cross-linked nanocomposites. First heating (left), first cooling (middle) and second heating (right).

S6 supplementary material shows the thermograms from which the residual weight values shown in Table 2 (manuscript) were obtained. These thermograms show that, apart from PCL/PSS, all chemically cross-linked nanocomposites present three distinct degradation events. The first event is

attributed to the evaporation of adsorbed water and/or ethanol (up to 5 wt%); the following event is attributed to the evaporation of silsesquioxanecages(around 20 wt%); and finally, the last event is due to the polymer degradation itself (around 55 wt%). The residue (around 20 wt%) composition may be described as silicon carbide and is generated by the mineralization of high molecular weight PSS, present in polysilsesquioxane nanoparticles. These results show that the organic and inorganic moieties degraded separately without influencing each other. Possibly, in the case of PCL/PSS, this behavior is also observed; however, with overlapping of the degradation events.

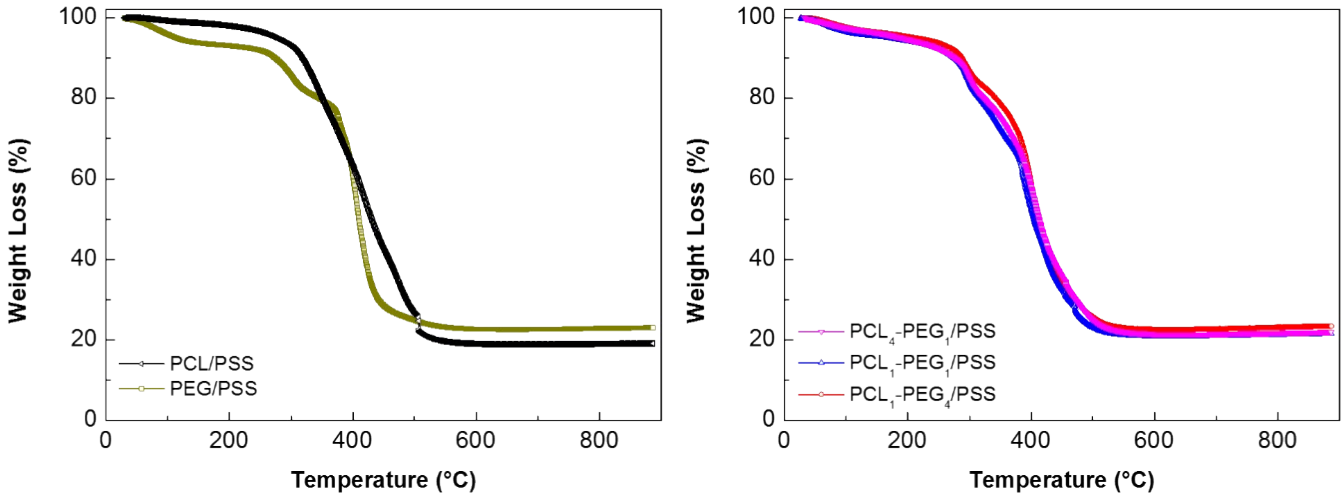

S6–Thermogravimetric analysis performed under argon atmosphere of the binary (left) and ternary (right) nanocomposites.

S7 supplementary material shows the water uptake of the hybrid nanocomposites as a function of time. There is a clear dependence of water swelling on PEG content due to the fact that PEG is the only hydrophilic component. As shown below, within 2 to 4 hours from water immersion, samples reached equilibrium. After that, the ternary nanocomposites began to show significant weight loss, while the binary nanocomposites were stable. In equilibrium, all samples preserved not only their spatial dimensions but also the mechanical stability and transparency. Weight loss during water exposure is due to PCL hydrolysis.

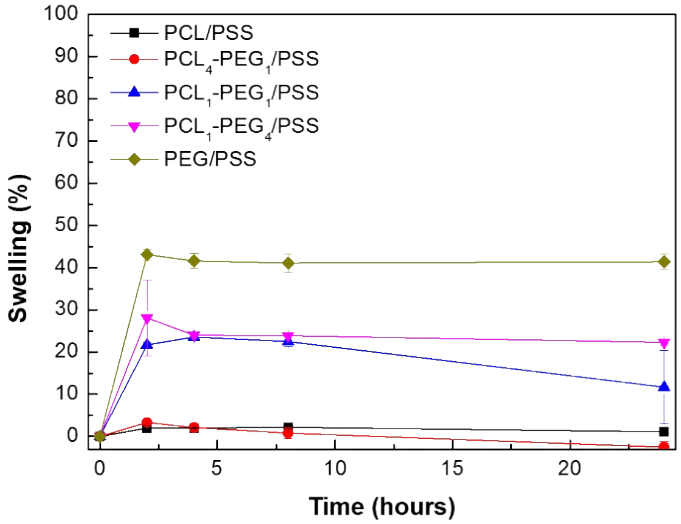

S7 – Water uptake of the binary and ternary chemically cross-linked nanocomposites as a function of time.

S8 supplementary material shows SEM micrographs and supplementary material S9 shows TEM micrographs of the binary (a; f) and ternary (b – e) hybrid nanocomposites. SEM images show that when PCL content is higher than 50% of the total organic components, larger polysilsesquioxane nanodomains may occur. This phenomenon is due to poor water mixing during hydrolysis-condensation of the triethoxysilane chain endsin the PCL rich hydrophobic matrix, and does not affect the overall behavior of the material. In contrast, TEM images show that with increasing PCL content, polysilsesquioxane nanodomains become smaller and less frequent at the nanoscale. S10 supplementary material shows the average distances and radius of these nanodomains as a function of PCL weight ratio in the hybrid nanocomposites. These measurements were taken from at least 150 nanoparticles using ImageJ® software.

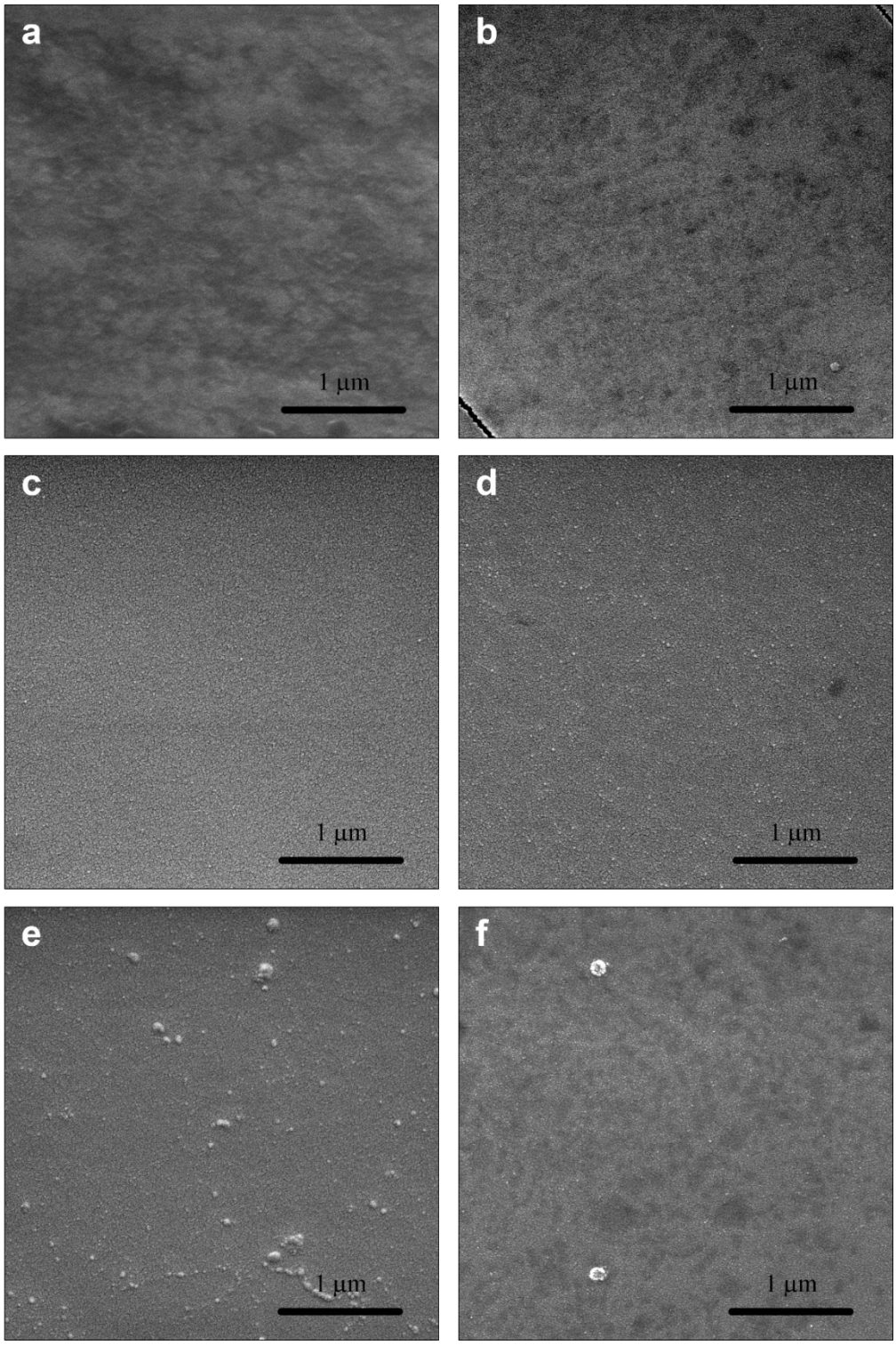

S8– Scanning electron micrographs of the crioultramicrotomed surfaces of PCG/PSS (a); PCL_1-PEG_4/PSS (b), PCL_2-PEG_3/PSS (c), PCL_3-PEG_2/PSS (d), PCL_4-PEG_1/PSS (e) and PCL/PSS (f) nanocomposites.

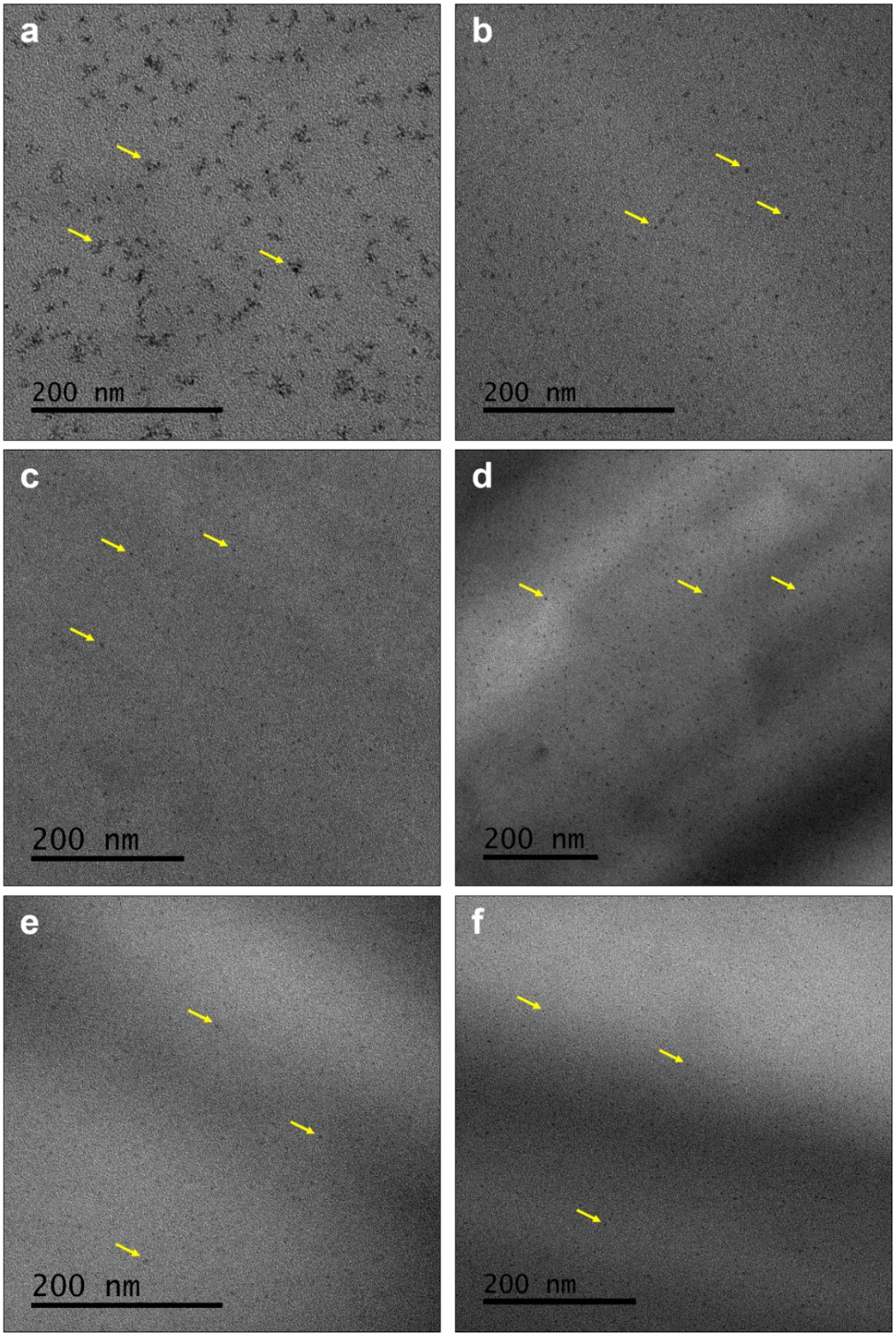

S9– Transmission electron micrographs of the ternary chemically cross-linked nanocomposites: PCG/PSS (a); PCL_1-PEG_4/PSS (b); PCL_2-PEG_3/PSS (c); PCL_3-PEG_2/PSS (d); PCL_4-PEG_1/PSS (e) and PCL/PSS (f). Polysilsesquioxane nanodomains are indicated by arrows.

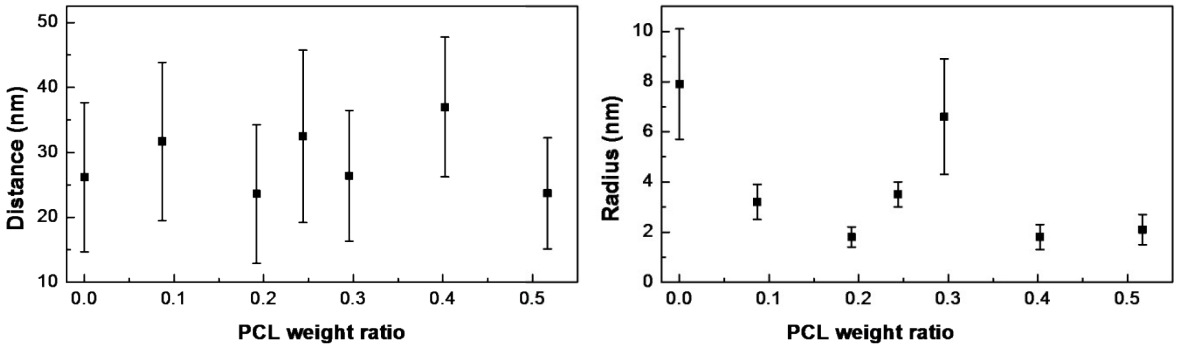

S10– Interparticle distances (left) and radii (right) of the polysilsesquioxane nanoparticles calculated from the TEM micrographs. Measurements are an average of at least 150 nanoparticles.

S11 supplementary material shows the electron energy loss spectrum (EELS) of the region from which the ESI-TEM (Figure 5b) image was obtained. The Si L-edge is clear and well defined which shows the results reliability. Moreover, the C K-edge which is also present, at 300 eV approximately, is an indication that both the organic and inorganic moieties occur within the imaged area

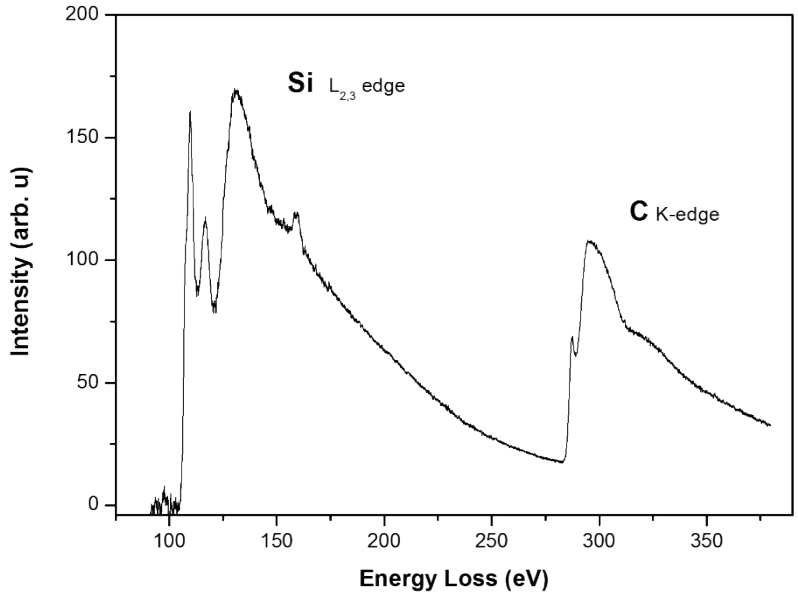

S11– Electron energy-loss spectrum at the Si $L_{2,3}$-edge taken from the PCL_1-PEG_1/PSS nanocomposite.

S12 supplementary material shows the evolution of the correlation distance d_{s2}, associated with peak 2, (Figure 5, manuscript) as a function of PCL weight ratio. As it can be observed, there is a 15% decrease of the d_{s2} value with increasing PCL content. This correlation distance is attributed to the amorphous high molecular weight polysilesquioxane at the spherical nanoparticles (Figure 4, manuscript).

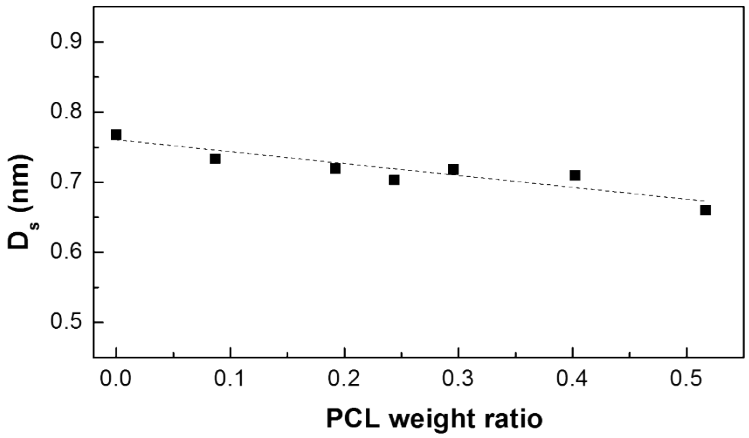

S12–Correlation distance d_{s2}, associated with peak 2, as a function of PCL weight ratio.

S13 supplementary material shows the small-angle scattering (SAXS) curves of the binary and ternary hybrid nanocomposites. These experiments were performed at $0.08 \leq q \leq 4.5$ nm^{-1}.
The high q-region, $q > 1$nm^{-1} has the same behavior as observed in peak 1 (Figure 5a). The low q-region, $q < 0.3$ nm^{-1}, shows a monotonic decrease of the scattering intensity which is characteristic of gel-like systems.

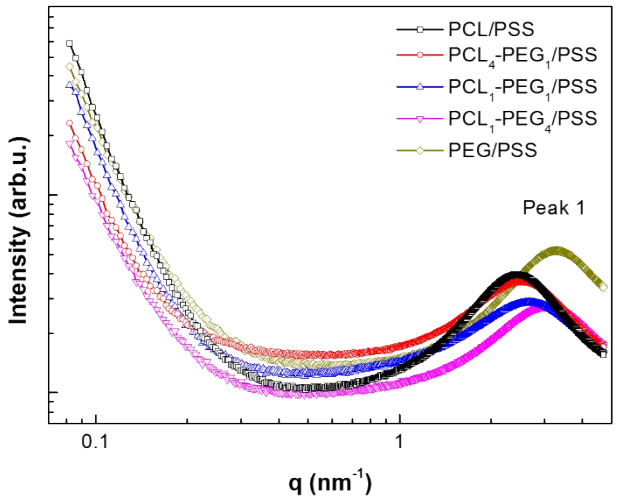

S13– Small-angle X-ray scattering curves of the binary and ternary hybrid nanocomposites obtained at q-range $0.08 \leq q \leq 4.5$ nm^{-1}. Peak 1 indicates the SAXS/WAXS overlapping region that holds the correlation distance of the ordered silsesquioxane/polymer networks.

Table S14 summarizes the set of ρ_i values obtained for the solution of Eq. (8) in the manuscript. It is worth to mention that, for the gradient descent optimization method performed in this work, only the ternary hybrids were considered. The sum of the minimum squared residues was 36.

S14 –Relative electronic densities of eachphase, ρ_i,present in the ternary hybrid nanocomposites where up: unbound polymer; cp: cross-linked polymer; np: polysilsesquioxane nanoparticle; sc: silsesquioxane cages.

Phase	ρ
np	9.3
sc	12.3
cl	8.2
up	3.2